Alterations in bile acid metabolizing gut microbiota and specific bile acid genes as a precision medicine to subclassify NAFLD

Short title: Bile acid metabolizing microbiota in NAFLD

Na Jiao[1, 2, $], Rohit Loomba[3, $,*], Zi-Huan Yang[1], Dingfeng Wu[2], Sa Fang[2], Richele Bettencourt[3], Ping Lan[1], Ruixin Zhu[2, *], Lixin Zhu[1, 4, *]

[1] Guangdong Institute of Gastroenterology, Guangdong Provincial Key Laboratory of Colorectal and Pelvic Floor Diseases, Department of Colorectal Surgery, the Sixth Affiliated Hospital, Sun Yat-sen University, Guangzhou 510655, P.R. China.

[2] Putuo people's Hospital, Department of Bioinformatics, Tongji University, Shanghai 200092, P.R.China.

[3] NAFLD Research Center, Division of Gastroenterology and Epidemiology, Department of Medicine, University of California San Diego, La Jolla, California 92093, United States.

[4] Department of Biochemistry, Genome, Environment and Microbiome Community of Excellence, The State University of New York at Buffalo, New York 14214, United States.

$ Equal contribution, * Corresponding authors

Grant support:

This work was supported by National Natural Science Foundation of China 81774152 (to RZ), 81770571 (to LZ), National Postdoctoral Program for Innovative Talents of China BX20190393 (to NJ), China Postdoctoral Science Foundation 2019M663252 (to NJ) and 2019M651568 (to DW), Natural Science Foundation of Shanghai 16ZR1449800 (to RZ), Fundamental Research Funds for the Central Universities

19ykzd01(to LZ) and 20kypy07(to NJ), the Guangzhou Science and Technology Plan Projects 201803040019 (to PL), Guangdong Province "Pearl River Talent Plan" Innovation and Entrepreneurship Team Project (2019ZT08Y464 to LZ) and the National Key Clinical Discipline of China, and Funds from the University at Buffalo Community of Excellence in Genome, Environment and Microbiome (GEM) (to LZ). RL receives funding support from NIEHS (5P42ES010337), NCATS (5UL1TR001442), and NIDDK (R01DK106419). The funders had no role in study design, data collection and analysis, decision to publish, or preparation of the manuscript.

Abbreviations:

baiA, 3α-hydroxysteroid dehydrogenase; **baiB**, bile acid-coenzyme A ligase; **baiCD**, 7α -hydroxy-3-oxo-D4-cholenoic acid oxidoreductase; **baiE**, bile acid 7α-dehydratase; **baiF**, bile acid coenzyme A transferase/hydrolase; **baiG**, primary bile acid transporter; **baiH**, 7beta-hydroxy-3-oxochol-24-oyl-CoA 4-desaturase; **baiI**, bile acid 7beta-dehydratase; **BAs**, bile acids; **BSH**, bile salt hydrolase; **FXR**, farnesoid X receptor; **HMM**, hidden Markov model; **HSDH**, hydroxysteroid dehydrogenase; **MAG**, metagenome-assembled genome; **NAFLD**, non- alcoholic fatty liver disease; **NASH**, non-alcoholic steatohepatitis; **WMS**, whole metagenome sequences.

Corresponding authors:

Rohit Loomba (roloomba@ucsd.edu)

NAFLD Research Center, Division of Gastroenterology and Epidemiology, University of California San Diego, 9500 Gilman Drive, MC 0887, La Jolla, CA 92093, United States.

Tel: 1-858-246-2201

Ruixin Zhu (rxzhu@tongji.edu.cn)

Putuo people's Hospital, Department of Bioinformatics, Tongji University, 1239 Siping Road, Shanghai 200092, P.R. China.

Tel: 86-21-6598-1041

Lixin Zhu (zhulx6@mail.sysu.edu.cn)

Guangdong Institute of Gastroenterology, Guangdong Provincial Key Laboratory of Colorectal and Pelvic Floor Diseases, Department of Colorectal Surgery, the Sixth Affiliated Hospital, Sun Yat-sen University, Guangzhou 510655, P.R. China.

Tel: 86-199-46256235

Disclosures:

The authors have declared that no competing interests exist.

Word count: 3216

Author's contributions:

LZ, RL and RZ conceived and designed the project. Each author has contributed significantly to the submitted work. NJ and RL drafted the manuscript. ZY, DW, SF, RB, PL, RZ and LZ revised the manuscript. All authors read and approved the final manuscript.

Availability of data and materials:

The datasets supporting the conclusions of this article are available in the NCBI's Sequence Read Archive repository (https://www.ncbi.nlm.nih.gov/bioproject/), under study accession number PRJNA373901, PRJNA420817, PRJEB1220 and PRJEB6070.

77

78 **Synopsis**

79 The microbial markers identified at the species/strain levels may be useful for

80 non-invasive diagnosis of NAFLD. The microbial differences in bile acid metabolism

81 and strain-specific differences among NAFLD microbiota highlight the potential for

82 precision medicine in NAFLD treatment.

83

84

85

Abstract

Background & Aims: Multiple mechanisms for the gut microbiome contributing to the pathogenesis of non-alcoholic fatty liver disease (NAFLD) have been implicated. Here, we aim to investigate the contribution and potential application for altered bile acid (BA) metabolizing microbe in NAFLD using whole metagenome sequencing (WMS) data.

Methods: 86 well-characterized biopsy-proven NAFLD patients and 38 healthy controls were included in the discovery cohort. Assembly-based analysis was performed to identify BA-metabolizing microbes. Statistical tests, feature selection and microbial interaction analysis were integrated to identify microbial alterations and markers in NAFLD. An independent validation cohort was subjected to similar analyses.

Results: NAFLD microbiota exhibited decreased diversity and microbial interactions. We established a classifier model with 53 differential species exhibiting a robust diagnostic accuracy (AUC=0.97) for dectecting NAFLD. Next, 8 important differential pathway markers including secondary BA biosynthesis were identified. Specifically, increased abundance of 7α-HSDH, baiA and baiB were detected in NAFLD. Further, 10 of 50 BA-metabolizing metagenome-assembled genomes (MAG)s, from *Bacteroides ovatus* and *Eubacterium biforme*, were dominant in NAFLD and interplayed as a synergetic ecological guild. Importantly, two subtypes of NAFLD patients were observed according to secondary BA metabolism potentials.

Elevated capability for secondary BA biosynthesis was also observed in the validation cohort.

Conclusions: We identified novel bacterial BA-metabolizing genes and microbes that may contribute to NAFLD pathogenesis and serve as disease markers. Microbial differences in BA-metabolism and strain-specific differences among patients highlight the potential for precision medicine in NAFLD treatment.

Keywords: NAFLD; gut microbiota; secondary BA synthesis; whole metagenome sequencing data

Introduction

Non-alcoholic fatty liver disease(NAFLD) has become one of the leading causes of liver disease worldwide, with the global prevalence estimated to be 24%.[1] NAFLD is expected to be the No. 1 cause for cirrhosis in the United States within a decade.[2]

The pathogenic mechanism of NAFLD remains unclear. The current multiple-hit hypothesis is that NAFLD is a consequence of a myriad of factors acting in a parallel and synergistic manner in individuals with genetic predisposition.[3] Factors such as insulin resistance, central obesity, environmental or nutritional factors, and gut microbiota, as well as genetic and epigenetic factors, are linked to its pathogenesis.[2, 4, 5]

Recently, the crosstalk between the gut and the liver is increasingly recognized, and many studies have reported dysregulated gut microbiota in NAFLD patients. [6-10] There are several potential mechanisms for the gut microbiota to influence NAFLD development. These effects are mediated by microbial components and metabolites, such as lipopolysaccharide, alcohol, and bile acid(BA).[11]

BA not only facilitate the digestion and absorption of fatty foods as detergent, they also act as important signaling molecules via nuclear receptors, such as farnesoid X receptor(FXR) and G protein coupled BA receptor(GPBAR1 or TGR5) to modulate hepatic BA synthesis, glucose and lipid metabolism. Recently, we observed suppressed BA-mediated FXR signaling in NAFLD liver and intestine, which is in harmony with increased secondary BA production. Furthermore, using 16S rRNA

data, we observed elevated abundance of secondary BA metabolizing related bacteria and pathways in the gut microbiome of NAFLD. [12] However, the 16S rRNA sequencing data has limited resolution which does not allow the identification of the species or an accurate functional analysis. [13]

Whole metagenome sequencing(WMS) allows us to achieve a satisfactory resolution of the microbiome. Earlier we have used the WMS data to characterize the gut microbiota in NAFLD patients with and without advanced fibrosis and identified 37 differential bacterial species, among which the abundance of *Escherichia coli* and *Bacteroides vulgatus* was increased in patients with advanced fibrosis and it's association with microbial metabolites.[9, 14-16] WMS data were also used to study the interactions between the gut microbiome and steatosis in obesity.[15, 17] However, a similar study is lacking for the comparison of the gut community between healthy and NAFLD subjects using WMS data, which is our goal in this study. Here we report the structural and functional characteristics of the gut microbiome in NAFLD, and its association with BA metabolism.

Results

Gut microbiota alterations between NAFLD patients and healthy controls

WMS data from 86 well-characterized biopsy-proven NAFLD patients and 38 healthy controls with similar characteristics (Table 1 and Table S1) were chosen to study the

structural and functional differences in gut microbiota between NAFLD patients and healthy controls. And we have confirmed that gender or age distribution did not account for the observed microbial differences in this study (Figure S1).

Compositional changes in NAFLD gut microbiota

We determined the microbial compositions of NAFLD and healthy controls using WMS data. Bacteroidetes, Firmicutes, Actinobacteria and Proteobacteria were the dominant phyla that collectively account for around 90% proportions in both groups (Figure S2A). NAFLD individuals had lower bacterial diversity than healthy controls (Figure S2B). Besides, significant compositional differences were observed between these two groups (Figure S2C).

To identify microbial markers that may distinguish NAFLD from healthy subjects, differential species were determined with Mann-Whitney U-tests. 53 species with FDR values < 0.1 were identified as differential species (Figure 1 & Table S2). Among these, 11 species were dominant in NAFLD patients, which mainly belong to Clostridia class, including E*ubacterium siraeum*, *Clostridium bolteae*, E. *coli* and *B.ovatus*, *B.stercoris* from Bacteroidia class. On the other hand, 42 species significantly reduced in NAFLD patients were mainly of Bacteroidia class, including, Bacteroides dorei, Alistipes shahii, and of Clostridia class, for instance, Eubacterium eligens, Eubacterium hallii, and Faecalibacterium prausnitzii. In addition, random forest (RF) model constructed with differential species achieved an AUC of 0.97 to detect NAFLD patients from controls (Figure S3).

Ecological structural changes in NAFLD gut microbiota

Furthermore, at whole-community level, microbial interaction analysis was performed to investigate potential changes in ecological structure. There were more species in healthy communities than those in NAFLD communities (167 nodes vs 141 nodes) though with similar amount of interactions. Then, we examined the "core community" (interactions with magnitudes > 0.4) of healthy and NAFLD groups, respectively. Considerable discrepancies existed in the "core community" of healthy and NAFLD (Figure 2A&B). In detail, the healthy "core community" was more complex, with 162 species and 565 interactions, compared to the NAFLD community with 81 species and 166 interactions. And the NAFLD community was separated into 8 isolated components, an indication of unstable microbial community. Among them, the major component harbored most species from Clostridia class, such as BA production bacteria, *C.bolteae* (node NO. 78), *C.clostridioforme* (node NO. 138) with increased proportion in NAFLD, while species from Bacilli class were dominant in the second major component. Besides, species with increased abundance in NAFLD patients (circle nodes in Figure 2B) were dominant in the "core community" and positively interacted with each other. Then, we looked into the top 20 hub species of "core community", respectively. 10 of them were common in both group, such as *C.bolteae*, *C.hathewayi*, *Dorea longicatena*, *Flavonifractor plautii*, which may play the role as the "keystone" to sustain the homeostasis (Figure 2C&D).

Functional changes in NAFLD gut microbiota

Microbial functional profiles were determined at pathway level using HUMAnN2 and 92 differential pathways were identified between the NAFLD and the healthy groups (Table S3). Similarly, we identified 8 important pathway features (Figure 3A) to build RF model (AUC=0.83) that could distinguish NAFLD patients from healthy subjects (Figure 3B). Most pathways were more represented in NAFLD microbiota than in controls. These pathways included secondary BA synthesis (ko00121) (Figure 3C), benzoate degradation (ko00362), biosynthesis of ansamycins (ko01051) and oxidative phosphorylation (ko00190) (Figure S4).

Novel genes and microbial genomes associated with secondary BA synthesis

The fact that the secondary BAs biosynthesis pathway was significantly elevated in NAFLD (Figure 3C) prompted us to examine the relevant BA metabolizing enzymes encoded by the microbiome. Taking advantage of the WMS data, we were able to quantify the gene abundance and to map these genes to specific microbial genomes.

Genes related to secondary BA synthesis

Bacterial genes directly involved in secondary BA synthesis catalyze the deconjugation, the oxidation and epimerization, or the multi-step 7α-dehydroxylation reactions (Figure 4A). Protein sequences of target enzymes were collected from Integrated Microbioal Genomes(IMG) database (Figure 4A).[18] High quality protein sequences were selected to construct hidden Markov models(HMMs), in order to

identify potential BA metabolizing enzymes.

The data (Figure 4B) showed that genes encoding 7-alpha-hydroxysteroid dehydrogenase(7α-HSDH), BSH and bile acid inducible operon (bai)A, baiB, baiCD, baiH were reletively more abundant than baiE, baiF and baiI. Importantly, significantly increased abundance of 7α-HSDH, baiA and baiB were observed in NAFLD compared to controls. These data were consistent with the pathway analysis results, and confirmed the increased secondary BA production in NAFLD.[12]

Novel identification of microbial genomes related to secondary BA synthesis using advanced bioinformatics

To identify the BA metabolizing microbial genomes, the metagenomic-assembled species(MAG) analysis was performed. Prevalent genes in the non-redundant gene catalog that presented in more than 5 samples were binned into 252 MAGs, which were considered to represent distinct microbial genomes. Among these, 50 MAGs that contain at least one gene encoding BSH, HSDH or bile acid inducible operons (Table S4) were defined as BA-metabolizing MAG. To obtain relatively complete microbial genomes, we re-assembled these 50 MAGs using high quality reads mapped to genes in each MAG.

Among these, 10 MAGs exhibited significantly increased abundance in NAFLD, while 18 MAGs were reduced in NAFLD (Figure 5A). Among the 10 MAGs elevated in NAFLD, 6 MAGs belong to Bacteroides (order Bacteroidales), including

B.vulgatus, *B.ovatus*, and *B.stercoris*. Other MAG genomes were assigned as *E.rectale* and *E.biforme* (order Clostridiales). BA-metabolizing MAGs with reduced abundance in NAFLD are mainly from *R.bromii*, *D.longicatena* and *B. dorei*. Furthermore, we explored the species' contributions of pathways in via HUMAnN2, and found that the pathway secondary bile acids biosynthesis were mainly encoded by *E.eligens* (48.3%) and *B.vulgatus* (26.2%)(Figure S5). This is consistent with the increased BA-metablizing MAGs belonging to species Bacteroides vulgatus and Eubacterium eligens.

For a better understanding of the BA metabolizing microbial community, microbial interactions analysis was performed with BA-metabolizing MAGs. In contrast to the situation where more interactions existed in healthy group on whole-community level, we found that the sub-network of BA-metabolizing MAG was more complex with considerable interactions in NAFLD than in controls (164 and 100 edges, respectively) (Figure 5B &C). In addition, most MAGs with higher proportions in NAFLD patients were hub nodes in both healthy and NAFLD BA-metabolizing communities and were positively interacted, such as *Bacteroides sp*. MAG001, *B.vulgatus* MAG007, *B.ovatus* MAG026, *B.vulgatus* MAG030 and *B.xylanisolvens* MAG117. These are likely "house-keeping" species for BA metabolism. In contrast, Bacteroides stercoris MAG003, an MAG not included in the healthy network, was highly elevated in NAFLD, ranked high in the NAFLD network, and positively interacted with the "house-keeping" BA metabolizing species. Similarly, *E.biforme*

MAG036 and MAG089, which exhibited the lowest hub score in healthy network, ranked the highest in NAFLD network.

In general, the observed species were represented by multiple MAGs. Here, *R.bromii* was represented by 7 MAGs, and *E.eligens* by 5 MAGs. However, only one of the 7 *R.bromii* MAG was significantly increased in NAFLD group, while 4 others showed decreased abundance (Table S5). Situations were similar in *B.vulgatus* (two of three increased) and *E.rectale* (one increased and two decreased). Unexpectedly, multiple MAGs of the same species were distributed in different modules both in healthy and NAFLD communities(Table S6). Apparently, these observations indicate that strains within the same species may function differently.

Different BA metabolizing potentials among NAFLD microbiota and emergence of two subtypes of NAFLD: High BA versus normal BA subtype

Although the average abundances of the secondary BA metabolism pathway and related genes were increased in NAFLD, we noticed that the abundances exhibited a broad distribution among NAFLD patients (Figure 3C and 4B). Many of the NAFLD microbiota exhibited BA metabolizing potentials similar to those of healthy controls. Based on the abundance of 3 differential BA-metabolizing genes (7α-HSDH, baiA and baiB), NAFLD patients were clustered into two subtypes: normal-BA subtype comprising 45 patients and high-BA subtype comprising 37 patients (Figure 6A), which was not related to the disease severity ($p=0.7$). The abundances of the 3 marker genes were all significantly higher in high-BA subtype, but were similarly represented

between normal-BA subtype and healthy control group (Figure 6B). In addition, we performed the PCA analysis based on the entire differential microbial enzymes and found that the normal-BA subtype and the healthy control group exhibited closer distance, as compared to the high-BA group (Figure 6C). In further characterization of the microbial profiles of the patterns of the normal-BA and high-BA groups, we identified 3 species (Table S7), 68 enzymes (Table S8) and 16 pathways (Table S9) that could distinguish the normal-BA subtype from the high-BA subtype, and, at the same time, could distinguish NAFLD from the healthy group. Based on the relative abundance of these differential features, the study subjects were clustered into three groups consistent with their BA metabolizing potentials. Features were also clustered into two groups (Figure S6). One group (including species Flavonifractor plautii, enzymes 2-dehydropantoate 2-reductase and glutamate 5-kinase and pathway glycosaminoglycan degradation etc.) exhibited elevated abundance in normal-BA subtype and reduced abundance in high-BA subtype. The other group (including species Escherichia coli and Ruminococcus bromii, enzymes glycerol dehydrogenase, agmatinase and pathway citrate cycle, phosphotransferase system etc.) exhibited an opposite distribution among the study groups.

Elevated secondary BA synthesis capability in the validation cohort of NAFLD

Similar analyses were performed with the validation dataset. The secondary BA synthesis genes 7α-HSDH, BSH,baiA, baiB, baiCD, baiF, and baiH were reletively

more abundant than baiE and baiI. Importantly, significantly increased abundance of most secondary BA synthesis genes were observed in NAFLD compared to controls (Figure S7).

As for BA metabolizing microbial genomes, we identified 13 MAGs, each carrying at least one gene encoding BSH, HSDH or bai operon. Among these, 9 MAGs exhibited a trend of increased abundance in NAFLD. Consistent with the discovery cohort, these 9 MAGs belonged to *B.vulgatus*, and *R. bromii*(Table S10). Statistical significance was not achieved for the increased abundances of the MAGs, likely due to the small sample size.

Discussion

In this study, we defined the structural and functional differences in gut microbiota between NAFLD and healthy subjects, at the resolutions of gene, species and strain. The current study is novel in using WGS data to compare the gut microbiota between NAFLD and healthy controls and underpinning the role of BA metabolizing microbiome in NAFLD, and potentially identifying two microbiota-derived subtypes of NAFLD that may have clinical implications for both biomarker as well as therapeutic development. Compared with the approach of 16S rRNA sequencing, WMS data allow direct function quantification and accurate taxa assignment of the entire gut microbiome, at the levels of species and strain. Out of the many differential representations of genes and species between NAFLD and healthy controls, one outstanding observation is the increased abundance of secondary BA metabolizing

genes and microbes in NAFLD and that BA metabolizing bacteria were dominant taxa in the gut of NAFLD. For the first time, we identified the genes and bacterial strains responsible for elevated secondary BA synthesis in NAFLD. Similarly, increased abundances of the BA metabolizing genes and bacterial species were observed in an independent validation cohort. Considering the profound impact of BA signaling on lipid and carbohydrate metabolism[19], the differential BA metabolizing genes and bacterial strains we identified may serve as novel therapeutic targets for NAFLD management.

We and others have reported elevated secondary BA production in NAFLD. [12, 20] In our previous study[12], we observed much increased secondary BAs in NAFLD serum and consistently, an elevated taurine metabolizing microbiota, an indication of increased BA metabolism in the gut. However, we did not observe any significant change in the abundance of those microbes that directly metabolize BA (that is, microbes encoding BSH, 7-alpha-HSDH and 7-alpha-dehydroxylase), likely because the 16S rRNA sequencing approach was not able to provide a sufficient resolution for functional analysis. With the advantage WGS data, the current study was able to provide convincing evidence at a satisfactory resolution, that secondary BA synthesis enzymes and microbes with secondary BA metabolizing potentials were indeed elevated in NAFLD gut microbiota. As secondary BAs are potent antagonistic ligands for FXR, data presented here is a strong support for the hypothesis that

elevated secondary BA synthesis by the microbiota contributes to NAFLD etiology.[12, 21]

Although on average NAFLD patients exhibited elevated BA metabolizing microbiota, and higher serum DCA (secondary BA) when compared to healthy controls, our data showed that elevated BA metabolizing microbiota was not a unanimous phenomenon in NAFLD. More than half of the NAFLD patients (45 out of 82) had a microbiota with normal BA metabolizing potential. Based on BA metabolizing potentials, our NAFLD patients can be clustered into two subtypes. This indicates that BA related pathomechanism does not apply to many NAFLD patients, in line with the current multi-hit hypothesis.[3] Besides the difference in BA metabolizing potentials, these two subtypes of the gut microbiota also exhibit different abundances in other genes, pathways, and bacterial species. It is interesting to note that NAFLD microbiota with higher BA metabolizing potentials also exhibited elevated representation of *E.coli*, a potent alcohol producer[6, 22], suggesting that the gut microbiota may impact NAFLD pathogenesis through multiple mechanisms in the same patient.

BA based therapies such as obeticholic acid has been shown to improve NASH. [23] However, the response rates to OCA in improvement of one-stage of fibrosis in the FLINT trial was 35% versus 19% in placebo.[24] It is plausible that NAFLD patients with altered BA subtype may be more likely to respond to BA based therapies

and those with a normal BA subtype should receive an alternate strategy paving the pay for a microbiome based precision medicine tool in NASH therapeutics.

Another outstanding observation in this study is that many strains of the same species are functionally different. Specifically, different strains of Bacteroides ovatus were clustered into different functional modules (modules 0, 2, 4 in healthy communities and modules 3, 4, 6 in NAFLD communities). It is also interesting to note that only one of the four observed strains of Bacteroides ovatus was significantly increased in NAFLD group. Similar observations were reported for *F. prausnitzii*[25, 26] and *E.coli*[27, 28], suggesting the genomic variability within a microbial species.[29] Some of the microbiome studies based on 16S rRNA platforms may need a re-evaluation because of this genomic variability.

It was interesting to note that 10 BA-metabolizing bacterial strains, including *B.stercoris, E.biforme*, and *R.bromii*, were elevated and were dominant strains in NAFLD microbiota. These BA-metabolizing strains belong to two different phylum. Zhao et al. proposed a concept in gut microbiota that a group of species that “exploit the same class of environmental resources in a similar way” may be considered as a “guild” in ecology[30] and members of a guild do not necessarily share taxonomic similarity, but they co-occur when adapting to the changing environment.[25] Similarly, the 10 BA-metabolizing strains may act as a synergetic guild to promote the secondary BA production in the NAFLD microbial community. There were more positive interactions among these 10 strains in NAFLD community than in healthy

384 community, indicating elevated capabilities of secondary BA production and
385 intensified competition among these secondary BA producers within the microbial
386 guild of NAFLD. It is likely that these strains are responsible for elevated secondary
387 BA production in NAFLD, contributing to NAFLD pathogenesis.[12] Among these
388 10 strains, MAG036，MAG089，and MAG003 with increased abundance and the
389 highest network importance in NAFLD may act as the “keystone” species[53], and
390 therefore, represent potential targets for intervention.
391 At the whole community level, the NAFLD gut microbiota exhibited significantly
392 reduced diversity compared to the healthy controls. In addition, much reduced
393 interactions among the members of the NAFLD gut microbiota were observed. With
394 less strains and sparse interactions, the gut microbial community in NAFLD is
395 relatively weak and unstable. Similarly, reduced biodiversity were reported in the gut
396 of obesity.[31] It is postulated that long-term dietary habit is the major cause for the
397 altered gut microbiota.[32] The biodiversity disaster in the gut of humans demands
398 immediate attention. The restoration of the gut microbial diversity may, at the same
399 time, prevent or cure many of the microbiota related diseases including NAFLD.
400 In summary, we identified specific genes and bacterial strains responsible for
401 elevated secondary BA production in NAFLD. These genes and strains may serve as
402 novel therapeutic targets for microbiome-based high-BA subtype of NAFLD. These
403 findings strongly support our hypothesis that elevated secondary BA synthesis
404 contributes to the development of NAFLD. In addition, our WGS study revealed the

heterogeneity of the gut microbiota among NAFLD patients highlighting the importance of personalized treatment for NAFLD. Our study also revealed many other microbial characteristics of the NAFLD that demands attention such as the much reduced diversity and the ecological guild in the gut of NAFLD.

Materials and Methods

Data information and preprocessing

Discovery dataset: The NAFLD datasets and relevant meta data(Sequence Read Archive, PRJNA373901) were described previously[9] comprising 86 biopsy-proven NAFLD patients. The healthy control dataset was from PRJEB6070[33], with 38 healthy individuals with BMI < 25. These subjects were chosen because of similar age and gender ratio compared to NAFLD patients to effectively reduce bias[34] (Table 1 & Table S1).

Validation dataset: 10 middle-aged NAFLD subjects [35] (PRJNA420817) were recruited to a diet trial and the initial baseline data before diet interventionwere used for this study. 11 healthy subjects from MetaHit Project[36](Sequence Read Archive, PRJEB1220) with similar age and gender ratio were chosen as controls (Table 1& Table S1).

All subjects provided a written informed consent and the study protocol was approved by Institutional Review Board (approval number:UCSD IRB11298) or registered at ClinicalTrials.gov with identifier: NCT02558530.

The KneadData(http://huttenhower.sph.harvard.edu/kneaddata) tool was used to ensure the data consisted of high quality microbial reads free from contaminants. The low quality reads were removed using Trimmomatic(SLIDINGWINDOW:4:15 MINLEN:75 LEADING:10 TRAILING:10). The remaining reads were mapped to the human genome(hg38) by bowtie2[37], and the matching reads were removed as contaminant reads from the host.

Gene-based taxonomic and functional profiling of gut microbiota

MetaPhlAn2[38] was used to identify the composition of gut microbial community and to assess the abundance of the prokaryotes within each sample. Species that failed to exceed 0.01% relative abundance in at least 20% samples were excluded.

The functional profiling of gut microbiome was determined by the HMP Unifiled Metabolic Analysis Network (HUMAnN2)[39]. In brief, high-quality metagenomic reads were mapped to the pangenomes of species identified with MetaPhlAn2 and these pangenomes have been pre-annotated by UniRef90 families. Reads failed to map to a pangenome were aligned to UniRef90 by translated search with DIAMOND[40]. Hits to UniRef90 are weighted according to alignment quality, sequence length and coverage. In this study, enzyme abundance was quantified by regrouping (summed) according to EC number and pathway abundance by regrouping (summed) genes in pathways against KEGG database.

Identification of genes required for secondary BA synthesis

To identify genes that encode enzymes catalyzing secondary BA synthesis, hidden Markov models (HMMs) of BA-related genes were constructed. Secondary BA synthesis mainly involves (1) deconjugation, (2) oxidation and epimerization and (3) multi-step 7α-dehydroxylation. Enzymes participating in these processes are bile salt hydrolase (BSH), hydroxysteroid dehydrogenase (HSDH) and enzymes required in the multi-step 7α-dehydroxylation (including baiA, baiB, baiCD, baiE, baiF, baiH and baiI).[18] Representative protein sequences of target enzymes were obtained from Integrated Microbioal Genomes (IMG) database[41]. High quality sequences were selected and aligned in Clustal Omega[42] before they were used to construct HMMs on full-length proteins via hmmbuild in HMMER(3.1b2)[43]. Model seed sequences were realigned to the model using hmmalign (default mode) before rebuilding models based on the obtained alignments until both model length and relative entropy per position were constant. Subsequently, all protein sequences in non-redundant gene catalog were screened (hmmsearch) for candidate protein sequences and sequences with hmmscore > lower quartile score and e-value less than 10-5 were identified as potential secondary BA synthesis associated genes.

Assembly-based microbial genomes

For functional analysis of the microbial genomes, we performed bin-based microbial genome assembly with the WMS data, including de nove assembly and non-redundant

human gut gene catalog construction, co-abundance clustering and determination of metagenome-assembled genomes (MAG), MAG-augmented assembly and taxonomic annotation.

De novo assembly and non-redundant human gut gene catalog construction

High-quality paired-end reads from each sample were used for de novo assembly with Megahit[44] into contigs of at least 500-bp length. Genes were predicted on the contigs with MetaGeneMark[45]. A non-redundant gene catalog related to NAFLD was constructed with CD-HIT[46] using a sequence indentity cut-off of 0.95, with a minimum coverage cut-off of 0.9 for the shorter sequences and 11,348,567 microbial genes were contained.

Co-abundance clustering and determination of MAG

Bowtie2 was used to align high quality reads to the non-redundant gene catalog. Aligned results were random sampled and downsized to 15 million per sample (FR-173, FR-719, FR-730, SRR4275396, SRR4275459, SRR4275469, SRR4275470 were excluded for not enough reads) to adjust for sequencing depth and technical variability. The soap.coverage script (available at: http://soap.genomics.org.cn/down/soap.coverage.tar.gz) was used to calculate gene-length normalized base counts and the gene abundance profiling was calculated as the average abundance of 30 times of repeated sampling. All the genes were clustered into MAG using MSPminer[47] based on their abundance with default

parameters.

MAG-augmented assembly and taxonomic annotation

We performed augmented assembly for target MAG. Briefly, the MAG- and sample-specific reads were derived by aligning all high-quality reads to the MAG gene contigs with Burrows-Wheeler Aligner (0.7.17)[48], followed by de novo assembly with SPAdes(3.13.0)[49] using k-mers from 21 to 55. CVtree3.0 web server[50] was used to identify the taxonomy of the MAGs, which applies a composition vector to perform phylogenetic analysis.

Statistic analysis

Differential features identification

Compositional features and functional features that present in at least 20% of the samples and with average relative abundance over 0.01% in each group were selected for further differential analysis. Differential features were identified by two-tailed Mann-Whitney U-tests adjusted by Benjamini-Hochberg. Features with an FDR value < 0.05 (FDR values < 0.1 for species) were identified as differential features. Then differential compositional and functional feature profiles were used to build random forest(RF) model using RandomForest package in R. Feature importance were estimated via gini importance and then the best model were rebuilt by adding features according to their importance ranks. Area Under the Receiver-Operator Curve(AUC) was used to measure the accuracy of the models.

Microbial interaction analysis

SparCC[51] was performed to construct compositionality-corrected microbial interactions network, which is capable of estimating correlation values from compositional data. Interactions were calculated with 100 refining interactions, after which statistical significance of each interaction was estimated with 1000 permutations. Only interactions with p value < 0.05 were included in downstream analysis and those interactions with magnitudes > 0.4 were included in the "core community". The importance of species in the community was calculated using Hyperlink-Induced Topic Search(HITS) algorithms in Python package 'networkx'. The networks were then visualized with Cytoscape[52] and module analysis was performed with ModuLand in Cytoscape.

Other statistics

Analysis of similarities (ANOSIM) was performed based on distance matrix for statistical comparisons of samples between groups or subtypes. P value was calculated using 9999 permutations. $p < 0.05$ indicates significant difference. Hetamap was plotted via "pheatmap" package in R, and features were clustered based on euclidean distance by "ward.D". Differential features among healthy, normal-BA and high-BA groups were identified with Dunn tests adjusted by Benjamini–Hochberg, and features with FDR values < 0.05 were determined as significant differential features.

References

[1] Younossi Z, Anstee QM, Marietti M, Hardy T, Henry L, Eslam M, George J, Bugianesi E. Global burden of NAFLD and NASH: trends, predictions, risk factors and prevention. Nat Rev Gastroenterol Hepatol 2018;15(1):11-20.

[2] Arab JP, Arrese M, Trauner M. Recent Insights into the Pathogenesis of Nonalcoholic Fatty Liver Disease. Annu Rev Pathol-Mech 2018;13:321-50.

[3] Tilg H, Moschen AR. Evolution of Inflammation in Nonalcoholic Fatty Liver Disease: The Multiple Parallel Hits Hypothesis. Hepatology 2010;52(5):1836-46.

[4] Piguet AC, Guarino M, Potaczek DP, Garn H, Dufour JF. Hepatic gene expression in mouse models of NAFLD after acute exercise. Hepatol Res 2019;49(6):637-52.

[5] Margini C, Dufour JF. The story of HCC in NAFLD: from epidemiology, across pathogenesis, to prevention and treatment. Liver Int 2016;36(3):317-24.

[6] Zhu L, Baker SS, Gill C, Liu WS, Alkhouri R, Baker RD, Gill SR. Characterization of Gut Microbiomes in Nonalcoholic Steatohepatitis (NASH) Patients: A Connection Between Endogenous Alcohol and NASH. Hepatology 2013;57(2):601-9.

[7] Michail S, Lin M, Frey MR, Fanter R, Paliy O, Hilbush B, Reo NV. Altered gut microbial energy and metabolism in children with non-alcoholic fatty liver disease. FEMS Microbiol Ecol 2015;91(2):1-9.

[8] Boursier J, Mueller O, Barret M, Machado M, Fizanne L, Araujo-Perez F, Guy CD, Seed PC, Rawls JF, David LA, Hunault G, Oberti F, Cales P, Diehl AM. The severity of nonalcoholic fatty liver disease is associated with gut dysbiosis and shift in the metabolic function of the gut microbiota. Hepatology 2016;63(3):764-75.

[9] Loomba R, Seguritan V, Li W, Long T, Klitgord N, Bhatt A, Dulai PS, Caussy C, Bettencourt R, Highlander SK, Jones MB, Sirlin CB, Schnabl B, Brinkac L, Schork N, Chen CH, Brenner DA, Biggs W, Yooseph S, Venter JC, Nelson KE. Gut Microbiome-Based Metagenomic Signature for Non-invasive Detection of Advanced Fibrosis in Human Nonalcoholic Fatty Liver Disease. Cell Metab 2017;25(5):1054-62 e5.

[10] Mouzaki M, Wang AY, Bandsma R, Comelli EM, Arendt BM, Zhang L, Fung S, Fischer SE, McGilvray IG, Allard JP. Bile Acids and Dysbiosis in Non-Alcoholic Fatty Liver Disease. PLoS One 2016;11(5):e0151829.

[11] Zhu L, Baker RD, Zhu R, Baker SS. Y Sequencing the Gut Metagenome as a Noninvasive Diagnosis for Advanced Nonalcoholic Steatohepatitis. Hepatology 2017;66(6):2080-3.

[12] Jiao N, Baker SS, Nugent CA, Tsompana M, Cai L, Wang Y, Buck MJ, Genco RJ, Baker RD, Zhu R, Zhu L. Gut microbiome may contribute to insulin

resistance and systemic inflammation in obese rodents: a meta-analysis. Physiological Genomics 2018;50(4):244-54.

[13] Sharpton SR, Ajmera V, Loomba R. Emerging Role of the Gut Microbiome in Nonalcoholic Fatty Liver Disease: From Composition to Function. Clin Gastroenterol Hepatol 2018;17(2):296-306.

[14] Caussy C, Hsu C, Lo MT, Liu A, Bettencourt R, Ajmera VH, Bassirian S, Hooker J, Sy E, Richards L, Schork N, Schnabl B, Brenner DA, Sirlin CB, Chen CH, Loomba R, Genetics of NiTC. Link between gut-microbiome derived metabolite and shared gene-effects with hepatic steatosis and fibrosis in NAFLD. Hepatology 2018;68(3):918-32.

[15] Caussy C, Loomba R. Gut microbiome, microbial metabolites and the development of NAFLD. Nat Rev Gastroenterol Hepatol 2018;15(12):719-20.

[16] Caussy C, Hsu C, Singh S, Bassirian S, Kolar J, Faulkner C, Sinha N, Bettencourt R, Gara N, Valasek MA, Schnabl B, Richards L, Brenner DA, Hofmann AF, Loomba R. Serum bile acid patterns are associated with the presence of NAFLD in twins, and dose-dependent changes with increase in fibrosis stage in patients with biopsy-proven NAFLD. Aliment Pharmacol Ther 2019;49(2):183-93.

[17] Hoyles L, Fernandez-Real JM, Federici M, Serino M, Abbott J, Charpentier J, Heymes C, Luque JL, Anthony E, Barton RH, Chilloux J, Myridakis A, Martinez-Gili L, Moreno-Navarrete JM, Benhamed F, Azalbert V, Blasco-Baque V, Puig J, Xifra G, Ricart W, Tomlinson C, Woodbridge M, Cardellini M, Davato F, Cardolini I, Porzio O, Gentileschi P, Lopez F, Foufelle F, Butcher SA, Holmes E, Nicholson JK, Postic C, Burcelin R, Dumas ME. Molecular phenomics and metagenomics of hepatic steatosis in non-diabetic obese women. Nat Med 2018;24(7):1070-80.

[18] Ridlon JM, Harris SC, Bhowmik S, Kang DJ, Hylemon PB. Consequences of bile salt biotransformations by intestinal bacteria. Gut Microbes 2016;7(1):22-39.

[19] Arab JP, Karpen SJ, Dawson PA, Arrese M, Trauner M. Bile acids and nonalcoholic fatty liver disease: Molecular insights and therapeutic perspectives. Hepatology 2017;65(1):350-62.

[20] Ferslew BC, Xie G, Johnston CK, Su M, Stewart PW, Jia W, Brouwer KL, Barritt ASt. Altered Bile Acid Metabolome in Patients with Nonalcoholic Steatohepatitis. Dig Dis Sci 2015;60(11):3318-28.

[21] Jiao N, Baker SS, Chapa-Rodriguez A, Liu W, Nugent CA, Tsompana M, Mastrandrea L, Buck MJ, Baker RD, Genco RJ, Zhu R, Zhu L. Suppressed hepatic bile acid signalling despite elevated production of primary and secondary bile acids in NAFLD. Gut 2018;67(10):1881-91.

[22] Clark DP. The fermentation pathways of Escherichia coli. FEMS Microbiol Rev 1989;5(3):223-34.

[23] Perazzo H, Dufour JF. The therapeutic landscape of non-alcoholic steatohepatitis. Liver Int 2017;37(5):634-47.

[24] Neuschwander-Tetri BA, Loomba R, Sanyal AJ, Lavine JE, Van Natta ML, Abdelmalek MF, Chalasani N, Dasarathy S, Diehl AM, Hameed B, Kowdley KV, McCullough A, Terrault N, Clark JM, Tonascia J, Brunt EM, Kleiner DE, Doo E, Network NCR. Farnesoid X nuclear receptor ligand obeticholic acid for non-cirrhotic, non-alcoholic steatohepatitis (FLINT): a multicentre, randomised, placebo-controlled trial. Lancet 2015;385(9972):956-65.

[25] Zhao L, Zhang F, Ding X, Wu G, Lam YY, Wang X, Fu H, Xue X, Lu C, Ma J, Yu L, Xu C, Ren Z, Xu Y, Xu S, Shen H, Zhu X, Shi Y, Shen Q, Dong W, Liu R, Ling Y, Zeng Y, Wang X, Zhang Q, Wang J, Wang L, Wu Y, Zeng B, Wei H, Zhang M, Peng Y, Zhang C. Gut bacteria selectively promoted by dietary fibers alleviate type 2 diabetes. Science 2018;359(6380):1151-6.

[26] Zhang C, Yin A, Li H, Wang R, Wu G, Shen J, Zhang M, Wang L, Hou Y, Ouyang H, Zhang Y, Zheng Y, Wang J, Lv X, Wang Y, Zhang F, Zeng B, Li W, Yan F, Zhao Y, Pang X, Zhang X, Fu H, Chen F, Zhao N, Hamaker BR, Bridgewater LC, Weinkove D, Clement K, Dore J, Holmes E, Xiao H, Zhao G, Yang S, Bork P, Nicholson JK, Wei H, Tang H, Zhang X, Zhao L. Dietary Modulation of Gut Microbiota Contributes to Alleviation of Both Genetic and Simple Obesity in Children. EBioMedicine 2015;2(8):968-84.

[27] Kaas RS, Friis C, Ussery DW, Aarestrup FM. Estimating variation within the genes and inferring the phylogeny of 186 sequenced diverse Escherichia coli genomes. Bmc Genomics 2012;13.

[28] Salipante SJ, Roach DJ, Kitzman JO, Snyder MW, Stackhouse B, Butler-Wu SM, Lee C, Cookson BT, Shendure J. Large-scale genomic sequencing of extraintestinal pathogenic Escherichia coli strains. Genome Research 2015;25(1):119-28.

[29] Mallick H, Ma SY, Franzosa EA, Vatanen T, Morgan XC, Huttenhower C. Experimental design and quantitative analysis of microbial community multiomics. Genome Biol 2017;18(1):228.

[30] Simberloff D, Dayan T. The Guild Concept and the Structure of Ecological Communities. Annu Rev Ecol Syst 1991;22:115-43.

[31] Menni C, Jackson MA, Pallister T, Steves CJ, Spector TD, Valdes AM. Gut microbiome diversity and high-fibre intake are related to lower long-term weight gain. Int J Obes (Lond) 2017;41(7):1099-105.

[32] Xu Z, Knight R. Dietary effects on human gut microbiome diversity. Br J Nutr 2015;113 Suppl:S1-5.

[33] Zeller G, Tap J, Voigt AY, Sunagawa S, Kultima JR, Costea PI, Amiot A, Bohm J, Brunetti F, Habermann N, Hercog R, Koch M, Luciani A, Mende DR, Schneider MA, Schrotz-King P, Tournigand C, Tran Van Nhieu J, Yamada T, Zimmermann J, Benes V, Kloor M, Ulrich CM, von Knebel Doeberitz M,

Sobhani I, Bork P. Potential of fecal microbiota for early-stage detection of colorectal cancer. Mol Syst Biol 2014;10:766.

[34] Cochran WG, Rubin DB. Controlling Bias in Observational Studies: A Review. Matched Sampling for Causal Effects 2006:30-57.

[35] Mardinoglu A, Wu H, Bjornson E, Zhang C, Hakkarainen A, Rasanen SM, Lee S, Mancina RM, Bergentall M, Pietilainen KH, Soderlund S, Matikainen N, Stahlman M, Bergh PO, Adiels M, Piening BD, Graner M, Lundbom N, Williams KJ, Romeo S, Nielsen J, Snyder M, Uhlen M, Bergstrom G, Perkins R, Marschall HU, Backhed F, Taskinen MR, Boren J. An Integrated Understanding of the Rapid Metabolic Benefits of a Carbohydrate-Restricted Diet on Hepatic Steatosis in Humans. Cell Metab 2018;27(3):559-71 e5.

[36] Qin J, Li R, Raes J, Arumugam M, Burgdorf KS, Manichanh C, Nielsen T, Pons N, Levenez F, Yamada T, Mende DR, Li J, Xu J, Li S, Li D, Cao J, Wang B, Liang H, Zheng H, Xie Y, Tap J, Lepage P, Bertalan M, Batto JM, Hansen T, Le Paslier D, Linneberg A, Nielsen HB, Pelletier E, Renault P, Sicheritz-Ponten T, Turner K, Zhu H, Yu C, Li S, Jian M, Zhou Y, Li Y, Zhang X, Li S, Qin N, Yang H, Wang J, Brunak S, Dore J, Guarner F, Kristiansen K, Pedersen O, Parkhill J, Weissenbach J, Meta HITC, Bork P, Ehrlich SD, Wang J. A human gut microbial gene catalogue established by metagenomic sequencing. Nature 2010;464(7285):59-65.

[37] Langmead B, Salzberg SL. Fast gapped-read alignment with Bowtie 2. Nat Methods 2012;9(4):357-9.

[38] Truong DT, Franzosa EA, Tickle TL, Scholz M, Weingart G, Pasolli E, Tett A, Huttenhower C, Segata N. MetaPhlAn2 for enhanced metagenomic taxonomic profiling. Nat Methods 2015;12(10):902-3.

[39] Franzosa EA, McIver LJ, Rahnavard G, Thompson LR, Schirmer M, Weingart G, Lipson KS, Knight R, Caporaso JG, Segata N, Huttenhower C. Species-level functional profiling of metagenomes and metatranscriptomes. Nat Methods 2018;15(11):962-8.

[40] Buchfink B, Xie C, Huson DH. Fast and sensitive protein alignment using DIAMOND. Nature Methods 2015;12(1):59-60.

[41] Markowitz VM, Chen IM, Palaniappan K, Chu K, Szeto E, Grechkin Y, Ratner A, Jacob B, Huang J, Williams P, Huntemann M, Anderson I, Mavromatis K, Ivanova NN, Kyrpides NC. IMG: the Integrated Microbial Genomes database and comparative analysis system. Nucleic Acids Res 2012;40(Database issue):D115-22.

[42] Sievers F, Higgins DG. Clustal Omega, Accurate Alignment of Very Large Numbers of Sequences. Multiple Sequence Alignment Methods 2014;1079:105-16.

[43] Johnson LS, Eddy SR, Portugaly E. Hidden Markov model speed heuristic and iterative HMM search procedure. Bmc Bioinformatics 2010;11:431.

[44] Li DH, Liu CM, Luo RB, Sadakane K, Lam TW. MEGAHIT: an ultra-fast single-node solution for large and complex metagenomics assembly via succinct de Bruijn graph. Bioinformatics 2015;31(10):1674-6.

[45] Zhu WH, Lomsadze A, Borodovsky M. Ab initio gene identification in metagenomic sequences. Nucleic Acids Res 2010;38(12):e132-32.

[46] Li W, Godzik A. Cd-hit: a fast program for clustering and comparing large sets of protein or nucleotide sequences. Bioinformatics 2006;22(13):1658-9.

[47] Plaza Onate F, Le Chatelier E, Almeida M, Cervino ACL, Gauthier F, Magoules F, Ehrlich SD, Pichaud M. MSPminer: abundance-based reconstitution of microbial pan-genomes from shotgun metagenomic data. Bioinformatics 2019;35(9):1544-52.

[48] Li H, Durbin R. Fast and accurate short read alignment with Burrows-Wheeler transform. Bioinformatics 2009;25(14):1754-60.

[49] Bankevich A, Nurk S, Antipov D, Gurevich AA, Dvorkin M, Kulikov AS, Lesin VM, Nikolenko SI, Pham S, Prjibelski AD, Pyshkin AV, Sirotkin AV, Vyahhi N, Tesler G, Alekseyev MA, Pevzner PA. SPAdes: a new genome assembly algorithm and its applications to single-cell sequencing. J Comput Biol 2012;19(5):455-77.

[50] Zuo GH, Hao BL. CVTree3 Web Server for Whole-genome-based and Alignment-free Prokaryotic Phylogeny and Taxonomy. Genom Proteom Bioinf 2015;13(5):321-31.

[51] Friedman J, Alm EJ. Inferring correlation networks from genomic survey data. PLoS Comput Biol 2012;8(9):e1002687.

[52] Shannon P, Markiel A, Ozier O, Baliga NS, Wang JT, Ramage D, Amin N, Schwikowski B, Ideker T. Cytoscape: a software environment for integrated models of biomolecular interaction networks. Genome Res 2003;13(11):2498-504.

[53] Wu DF, Jiao N, Zhu RX, Zhang YD, Gao WX, Fang S, Li YC, Cheng SJ, Tian C, Lan P, Loomba R, Zhu LX. Identification of the keystone species in non-alcoholic fatty liver disease by causal inference and dynamic intervention modeling. bioRXiv 2020; doi: 10.1101/2020.08.06.240655.

Table1 Characteristics of the cohort included in this study

	Discovery cohort		Validation cohort	
	NAFLD	Control	NAFLD	Control
Sample Size	86	38	10	11
Age	51.56±12.67	55.71±12.75	53.7±3.65	56.18±6.65
BMI	30.25±5.46	23.03±1.88	34.1±1.2	23.19±0.92
Gender(F%/M%)	44.19/55.81	50.00/50.00	20.00/80.00	63.63/36.36
AST(U/L)	32.5±29.96	NA[$]	30.8±2.4	NA
LDL cholesterol(mg/dL)	116±37.12	NA	52.25±5.41[#]	NA
HDL cholesterol (mg/dL)	46±15.97	NA	20.36±1.26	NA
Triglycerides(mg/dL)	129±95.70	NA	50.45±7.21	NA
Total cholesterol(mg/dL)	191.5±43.39	NA	95.90±5.41	NA

Data are presented as median±SD

$ NA, not available. The control groups included healthy individuals (Ref 33 and 36)

The data are converted form mmol/L to mg/dL.

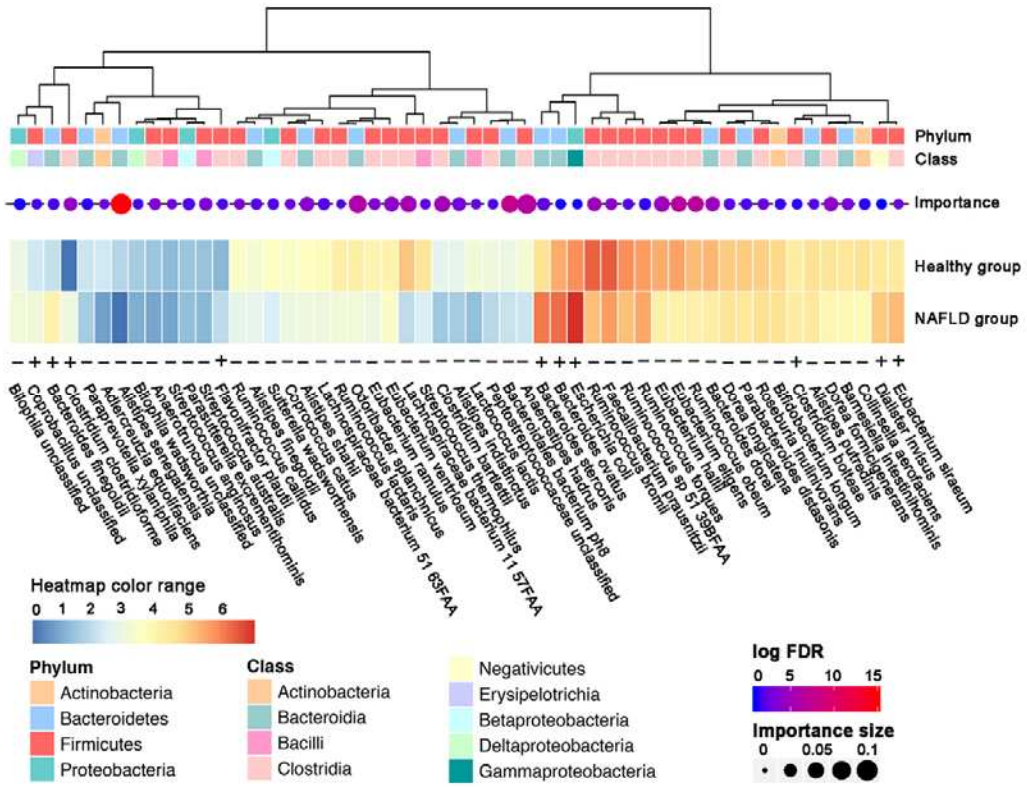

Figure 1. The differential species distinguishing NAFLD patients from healthy controls. Differential species were selected by statistical tests (two-tailed Mann-Whitney U-tests adjusted by Benjamini–Hochberg). Furthermore, the

728 importance of the species that distinguish NAFLD patients from healthy controls was
729 evaluated with random forest model. The heatmap shows the relative abundance
730 (log-transformed) of the differential species in the NAFLD and the healthy groups,
731 the size of the dots is proportional to the importance and the color shows the FDR
732 value (-log-transformed). "+" indicates increased abundance while "-" indicates
733 decreased abundance in NAFLD.

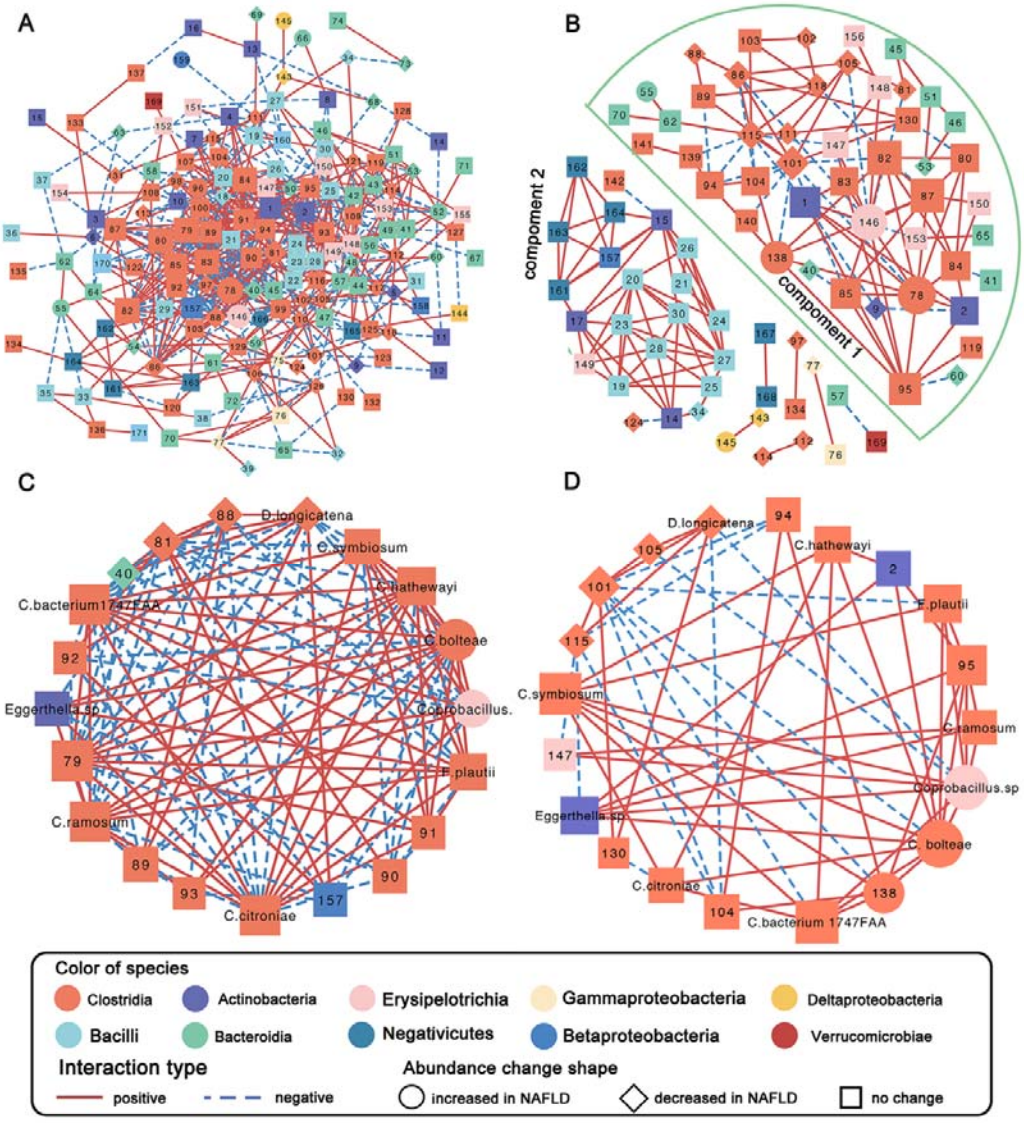

734

735 Figure 2. Microbiota "core community" in healthy controls (A&C) and NAFLD
736 patients (B&D). The microbial interactions were calculated using SparCC with 100
737 refining interactions, and p value of each interaction is approximated with 1000

permutations. Only interactions with p value < 0.05 and interactions with magnitudes > 0.4 were included in the "core community". The species were colored according to the class they belong to and the node size indicates the hub score in their community. Sub-network of top 20 hub nodes in healthy community (C) and NAFLD community (D) was also plotted. The nodes indicated by species name were common species in both sub-networks.

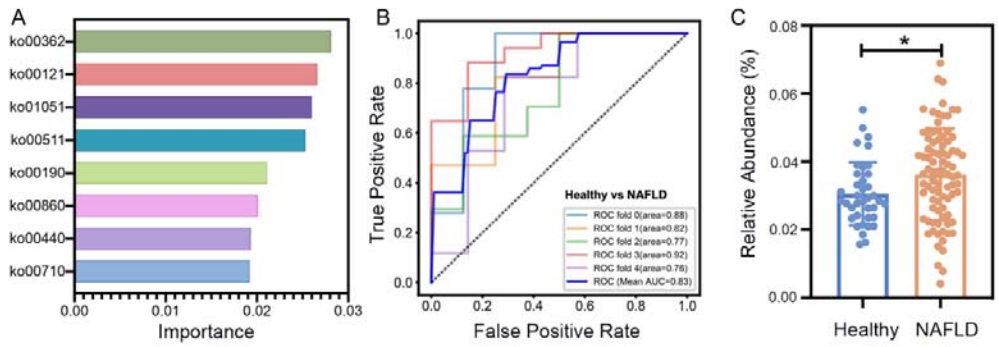

Figure 3. The differential pathway markers distinguishing NAFLD patients from healthy controls. Differential pathways were selected by two-tailed Mann-Whitney U-tests adjusted by Benjamini–Hochberg. Pathways with FDR values < 0.05 were included. Important differential pathway markers were then identified with random forest model and with the top 8 important pathways, the model achieved the highest AUC value. (A). The importance of pathways evaluated in NAFLD with the random forest model. (B). The AUC curve of random forest model with the top 8 important pathways. (C). The abundance of secondary A biosynthesis pathway (ko00121) in the healthy and the NAFLD groups. Values are the mean±SD. * indicates FDR<0.05.

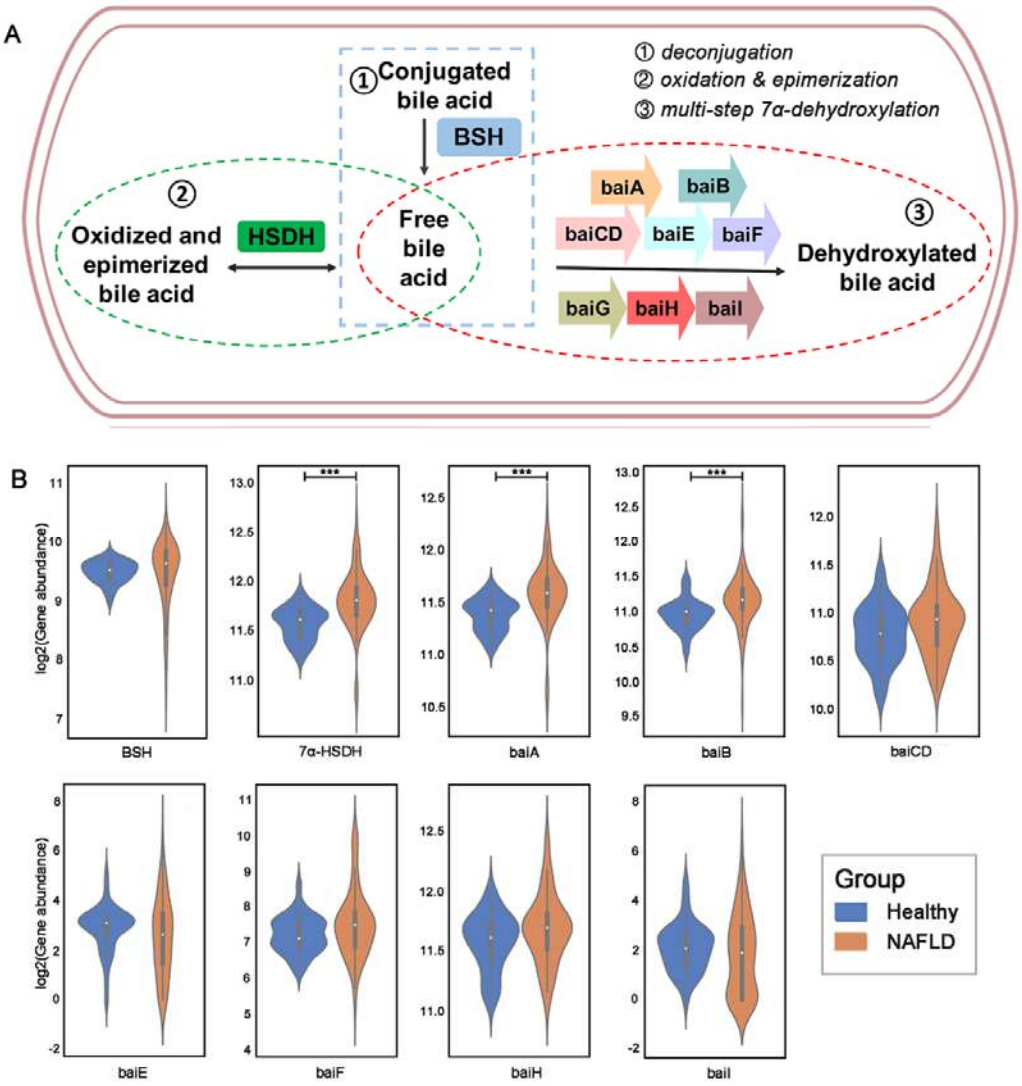

754

755 Figure 4. The abundance of the bacterial genes related to secondary bile acid
756 synthesis. (A) Genes responsible for secondary bile acid biosynthesis can be grouped
757 into 3 categories: (1) deconjugation, (2) oxidation and epimerization and multi-step
758 7α-dehydroxylation. (B) Gene abundance in health and NAFLD groups. Differences
759 were identified by two-tailed Mann-Whitney U- tests adjusted by
760 Benjamini–Hochberg. BSH: bile salt hydrolase; HSDH: hydroxysteroid
761 dehydrogenase; baiA, 3α-hydroxysteroid dehydrogenase; baiB, bile acid-coenzyme A
762 ligase; baiCD, 7α -hydroxy-3-oxo-D4-cholenoic acid oxidoreductase; baiE, bile acid
763 7α- dehydratase; baiF, bile acid coenzyme A transferase/hydrolase; baiG, primary bile

764 acid transporter; baiH, 7beta-hydroxy-3-oxochol-24-oyl-CoA 4-desaturase; baiI, bile
765 acid 7beta-dehydratase. *** indicates FDR<0.001.

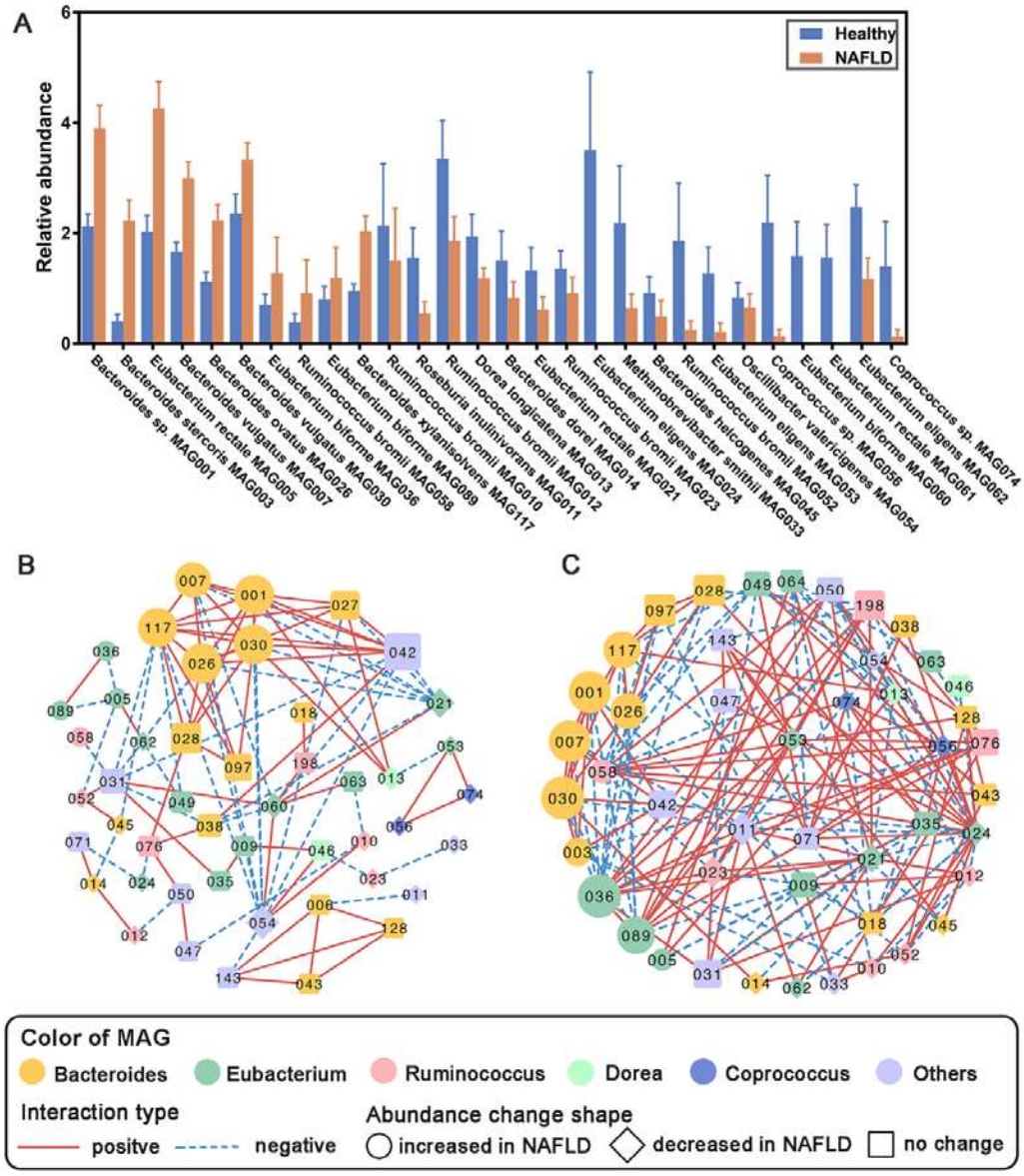

766

767 Figure 5. BA metabolizing MAG in NAFLD and healthy subjects. (A) MAG
768 exhibiting differential abundance between healthy controls and NAFLD patients.
769 Differential MAG were selected by two-tailed Mann-Whitney U- tests adjusted by
770 Benjamini–Hochberg. MAG with FDR values < 0.1 were included. Values are mean
771 ± SEM. Interaction network for BA metabolising MAG community in healthy
772 controls (B) and NAFLD patients (C). Microbial interactions were calculated using

773 SparCC with 100 refining interactions, and p value of each interaction is
774 approximated with 1000 permutations. Only interactions with p value < 0.05 were
775 included.

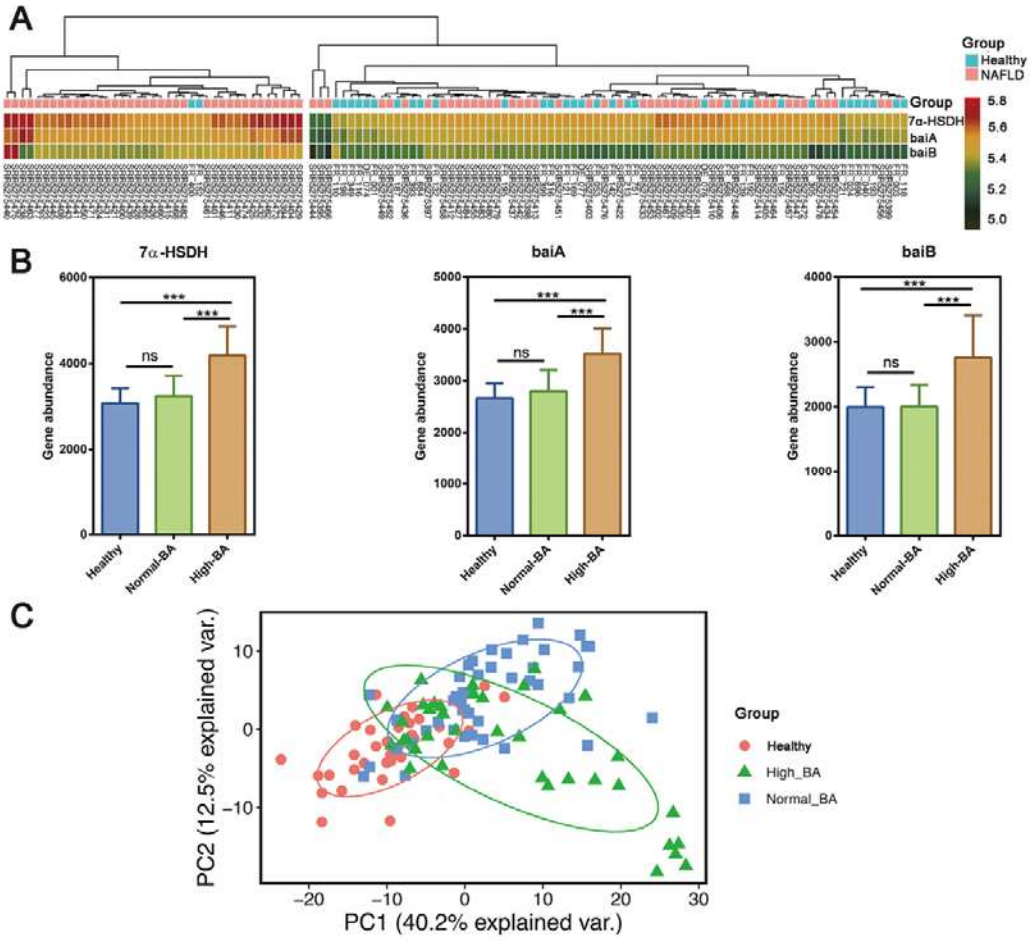

776

777 Figure 6. Subgroups of NAFLD patients with different abundances of the secondary
778 BA synthesis genes. (A) NAFLD patients were clustered into two subgroups:
779 normal-BA subgroup and high-BA subgroup according to the abundances of 3
780 differential secondary BA synthesis genes. (B) Comparison of the abundances of 3
781 differential secondary BA synthesis genes among healthy control, normal-BA and
782 high BA groups. They were all significantly increased in high-BA subgroup, but was
783 not different between normal-BA subgroup and healthy group (Dunn tests adjusted by
784 Benjamini–Hochberg). (C) PCA plot based on the differential enzymes. Subjects were

785 clustered according to the secondary BA metabolizing potentials ($p < 0.001$ with

786 ANOSIM analysis). Values are mean±SD. *** indicates FDR<0.001.